Solar Energy Materials and Solar Cells 185 (2018) 439–444

Contents lists available at ScienceDirect

Solar Energy Materials and Solar Cells

journal homepage: www.elsevier.com/locate/solmat

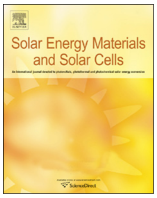

# Enhanced optoelectronic conversion in diamond-wire sawing multi-crystalline silicon solar cells through nanotexture-induced photon management

Wenhui Lu[a,b,*], Xiaoyong Qiu[b,c], Qingguo Zhao[b,c], Bo Lu[b], Yifeng He[b], Fangfang Luo[a], Tao Pang[a], Xiaofei Li[b], Shuai Zhang[a]

[a] *Department of Applied Physics, College of Science, Huzhou University, Huzhou, Zhejiang 313000, PR China*
[b] *Zhejiang Beyondsun PV Co., Ltd, Huzhou, Zhejiang 313008, PR China*
[c] *Zhejiang Trunsun Solar Co., Ltd, Huzhou, Zhejiang 313008, PR China*

ARTICLE INFO

*Keywords:*
DWS mc-Si solar cells
Nanotexturing
Reactive ion etching
Photon management
Enhanced optoelectronic conversion

ABSTRACT

Nanotextured diamond-wire sawing (DWS) multi-crystalline silicon (mc-Si) solar cells are successfully fabricated on an industrial scale. The nanotextures are achieved through reactive ion etching (RIE). By introducing the RIE-nanotextures, the DWS mc-Si solar cells with aluminum back-surface field (Al-BSF) structure exhibit an enhanced optoelectronic conversion, and high power conversion efficiency (*PCE*) of up to 19.50%. This enhanced optoelectronic conversion is attributed to nanotexture-induced photon management effect, including both efficient reflection reduction and absorption enhancement, and which offset over the increased recombination of charge carriers. The DWS mc-Si solar cells are promising for industrial production due to the low raw material cost, high PCE, and manufacturing processes compatible with the existing production lines.

## 1. Introduction

Recently, photovoltaic (PV) materials and PV devices have attracted considerable interests since solar cells offer a practical approach to convert solar energy into electricity directly. Multi-crystalline silicon (mc-Si) solar cells have occupied 65–75% of the PV market. However, the price of mc-Si solar cells still needs to be further reduced in order to compete with the fossil fuel based energy. In a typical mc-Si solar cell, the material cost of silicon wafer is about 63% of the overall cost of fabricating solar cells [1]. Since crystalline silicon is a weak absorber [2], and the commercial mc-Si solar cells adopt 180–200 μm thick active layer to adequately absorb the sun light. Furthermore, slicing mc-Si ingot into mc-Si wafer causes a material loss of more than 50% if the conventional slurry wire sawing (SWS) technique is used.

Currently, diamond-wire sawing (DWS) technique [3,4] is being applied to the slicing of mc-Si ingot. DWS technique has several advantages such as a three-times faster sawing speed, low material loss, recyclable sawing silicon powder, and reduced material cost of USD 4.5–8 cents per piece for mc-Si wafer compared to that of the conventional SWS process. It is obvious that DWS is an efficient way to produce low cost mc-Si wafers for solar cells. Unfortunately, the light reflection loss of DWS mc-Si solar cells with conventional wet acidic etching (WAE) process [5] is 3–5% higher than that of SWS mc-Si solar cells, due to less surface mechanical damage and smooth surface of DWS mc-Si wafers. Conventionally prepared DWS mc-Si solar cells are less effective to convert solar energy.

Many new texturing technologies [6,7] may be available for DWS mc-Si solar cells, such as metal catalysed chemical etching (MCCE) [8–10], reactive ion etching (RIE) [11,12], atmospheric pressure $F_2$ based dry etching [13–15], laser etching [16] and plasma immersion ion implantation [17,18]. MCCE is a low cost texturing process and has been reported for texturing of DWS mc-Si solar cells [19–21]. However, MCCE needs to use heavy metal ions [22] such as $Ag^+$, which lead to environmental pollution. RIE is another effective surface nanotexturing process for mc-Si solar cells [11,12]. RIE processing mc-Si solar cells can achieve high power conversion efficiency (*PCE*) [12,23]. In the RIE process, the product of $Si_xO_yF_z$ presents a self-mask effect [24], facilitating the formation of nanotextured surface on crystalline silicon. Even though DWS mc-Si wafers have less surface mechanical damage and smooth surface, a uniform nanotextured surface can be obtained by RIE process due to the etching mechanism of the self-mask. Thus, RIE process would be very suitable for the surface texturing of DWS mc-Si solar cells. As a result, it is essential to demonstrate the application potential of RIE process for low cost DWS mc-Si solar cells as compared

---

* Corresponding author at: Department of Applied Physics, College of Science, Huzhou University, Huzhou, Zhejiang 313000, PR China.
*E-mail address:* whlv2016@189.cn (W. Lu).

https://doi.org/10.1016/j.solmat.2018.06.001
Received 11 January 2018; Received in revised form 31 May 2018; Accepted 1 June 2018

to that of conventional WAE process [5], and to understand the optoelectronic conversion process in the RIE-nanotextured DWS mc-Si solar cells.

In this work, RIE-nanotextured DWS mc-Si solar cells with aluminum back-surface field (Al-BSF) architecture have been fabricated on an industrial scale. The optoelectronic conversion of the RIE-nanotextured DWS mc-Si solar cells are investigated as compared to that of conventional WAE process. By the reflection spectra, transmittance spectra and quantum efficiency, we identify that photon management through the surface nanotexturing plays a critical role on optoelectronic conversion performance of RIE-nanotextured DWS mc-Si solar cells.

## 2. Experiment

P-type DWS mc-Si (200 ± 20 µm thick, 1–3 Ω cm) wafers with a standard size of 156.75 × 156.75 $mm^2$ were used in this work. The wafers were first processed with conventional wet acidic etching [5] to produce micropit structures. The wafers were then treated with RIE process [25] to generate nanotextures. In the RIE process, the gas mixture of $SF_6$, $O_2$ and $Cl_2$ with flow ratio of 17:24:10 was employed to etch DWS mc-Si wafers at a pressure of 30 Pa. After the RIE process, the DWS mc-Si wafers were cleaned using a BOE/$H_2O_2$ solution (BOE, mixed aqueous solution of $NH_4F$ and HF) and HF solution, respectively. The resulting RIE-nanotextures on the surface of the mc-Si wafers were characterized by scanning electron microscope (SEM) (Hitachi, S3400N). The hemispherical reflectance spectra and transmittance spectra of processed DWS mc-Si wafers were obtained by UV–visible-near infrared spectroscopy with an integrating sphere attachment (Shimadzu, UV-2600).

The two series of DWS mc-Si solar cells without and with RIE-nanotextures (500 cells for each series) were prepared using standard industrial processes [26,27]. All cells were Al-BSF architecture with 5 bus-bars. The fabrication processes of the DWS mc-Si solar cells were illustrated in Fig. 1. After surface texturing, $POCl_3$ based tube diffusion was employed to form p-n junction emitter. In the diffusion process, the sheet resistances of the emitter of all cells were controlled in the range of 100 ± 5 Ω/□. The high sheet resistance is beneficial to diminish the surface and bulk recombination of photo-generated carriers in the nanotextured emitter [8,28]. Then the phosphorous doping layer of wafer back surface and wafer edge were removed by wet etching in a HF/$HNO_3$ solution. The $SiN_x$ antireflection/passivation coating was deposited by plasma-enhanced chemical vapor deposition. The thickness of the $SiN_x$ coating for all cells was about 80 nm. Finally, Ag and Al paste was subsequently screen printed on both the front and rear surfaces to form top/bottom electrodes. The performance of the DWS mc-Si solar cells without and with RIE-nanotextures were characterized by standard solar simulated light illumination (AM 1.5 G, 100 mW/$cm^2$) (Berger Lichttechnik, PSS10), and the corresponding quantum efficiency (QE) were identified at solar cell spectral response measurement system (Zolix, SCS100-Std).

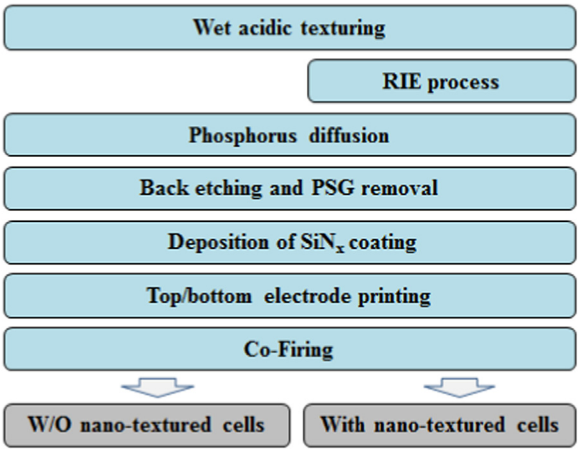

**Fig. 1.** The fabrication processes of the DWS mc-Si solar cells without and with RIE-nanotextures.

## 3. Results and discussion

Figs. 2**(a)** and 2**(b).** shows the SEM images of surface morphology of DWS mc-Si wafers processed by WAE. Some micropits can be observed on the mc-Si wafer. However, both the number and density of the micropits are found to be lower than that of the WAE processing SWS mc-Si wafers [5], which can be ascribed to less surface mechanical damage and smooth surface of DWS mc-Si wafers. High packing density RIE-nanotextures with pseudo-pyramidal shape are found on the surface of DWS mc-Si wafers after the RIE process and BOE/$H_2O_2$ modification, as shown in Figs. 2**(c)** and 2**(d)**. The pseudo-pyramidal configuration is easy to achieve conformally deposition of $SiN_x$ film on the nanotextures [9]. The size of pseudo-pyramids is about 250–420 nm, which can efficiently diffract sun light, and consequently suppresses the surface reflection.

The hemispherical reflection spectra of the RIE-nanotextured DWS mc-Si wafer are shown in Fig. 3**(a).** as compared to the surface of the DWS mc-Si wafer without RIE-nanotextures. The DWS mc-Si wafers decorated with RIE-nanotextures exhibit a lower optical reflection in the range of 300–1100 nm. After the deposition of $SiN_x$ coating on the surface of DWS mc-Si wafer, the hemispherical reflection is further reduced. In addition, the effective transmittance spectra $T_E(\lambda)$ are obtained using equation $T_E(\lambda) = T_M(\lambda)/(1 - R_M(\lambda))$, where $R_M(\lambda)$ is the measuring reflectance, and $T_M(\lambda)$ is the measuring transmittance. As shown in Fig. 3**(b)**, a reduced optical transmission is observed in the range of 900–1100 nm, after the introduction of RIE-nanotextures. To further evaluate the light-trapping capability of the nano-textured DWS mc-Si wafer, the reflection loss ratio $\eta_R$ in the range of 300–1100 nm and effective transmittance loss ratio $\eta_T$ in the range of 900–1100 nm are described by the following Eqs. (1) and (2), respectively.

$$\eta_R = \frac{\int_{300nm}^{1100nm} R_M(\lambda)\frac{I_{AM1.5G}(\lambda)}{(hc/\lambda)}d\lambda}{\int_{300nm}^{1100nm} \frac{I_{AM1.5G}(\lambda)}{(hc/\lambda)}d\lambda} \tag{1}$$

$$\eta_T = \frac{\int_{900nm}^{1100nm} T_E(\lambda)\frac{I_{AM1.5G}(\lambda)}{(hc/\lambda)}d\lambda}{\int_{900nm}^{1100nm} \frac{I_{AM1.5G}(\lambda)}{(hc/\lambda)}d\lambda} \tag{2}$$

Where $\lambda$ is the wavelength, $h$ is the Planck constant, and $c$ is the light speed, and $I_{AM1.5G}$ is the AM1.5 G solar spectrum [29], while the results obtained are summarized in Table 1. After introducing the RIE-nanotextures, the reflection loss ratio of the $SiN_x$ coating DWS mc-Si wafer is reduced from 8.05% to 3.19% in the range of 300–1100 nm. The results demonstrate that the RIE-nanotextures can effectively reduce surface reflection of DWS mc-Si wafer. On the other hand, the effective transmittance loss ratio of the $SiN_x$ coated DWS mc-Si wafer is also reduced from 12.02% to 6.59% in the range of 900–1100 nm. It can be concluded that the RIE-nanotextures can effectively increase the absorption path of photons, thus enhance absorption in the DWS mc-Si wafer. Based on the comparative analysis of the measured results in Fig. 3, it can be concluded that the RIE-nanotextures on the surface of DWS mc-Si wafers play a critical role in both the efficient reflection reduction and absorption enhancement, which is attributed to the nanotexture-induced photon management effect.

Fig. 4. shows the performance parameter distributions of the DWS mc-Si solar cells without and with RIE-nanotextures. From these statistical results, it can be clearly seen that the short-circuit current density ($J_{sc}$) of the RIE-nanotextured cells is significantly higher than that of the cells without the RIE-nanotextures. However, the open-circuit voltage ($V_{oc}$) of the RIE-nanotextured cells is lower than that of the cells without RIE-nanotextures. In addition, the RIE-nanotextured cells